ACS OMEGA

http://pubs.acs.org/journal/acsodf

Article

Magnetic Control-Enhanced Lateral Flow Technique for Ultrasensitive Nucleic Acid Target Detection

Wen Ren and Joseph Irudayaraj*

Cite This: *ACS Omega* 2022, 7, 29204−29210

Read Online

ACCESS | Metrics & More | Article Recommendations

ABSTRACT: In this work, a lateral flow (LF)-based detection strategy termed magnetic control-enhanced LFA (MCLF) was proposed to detect nucleic acid sequences at attomolar sensitivity. In the proposed MCLF method, magnetic controllers which are magnetic nanoparticles modified with antibodies against the labels on capture sequences were used to interact with the unreacted labeled capture sequence (CS-label) to improve the detection limit. By regulating the movement of magnetic probes (magnetic controllers) with a simple magnet under the lateral flow strip, the movement of magnetic probes bounded with unreacted CS-label in the sample flow could be reduced. Therefore, the target sequence-containing sandwich structures will arrive at the test zone prior, to interact with the recognition ligands, whereby the capture efficiency of the sandwich structures could be increased because the unreacted capture sequences at the test zone will be reduced. With the colorimetric signal from gold nanoparticle-based probes, the proposed MCLF technique could recognize as low as 100 aM of DNA target sequences by naked eyes, and the responding range of MCLF is from 100 aM to 10 pM.

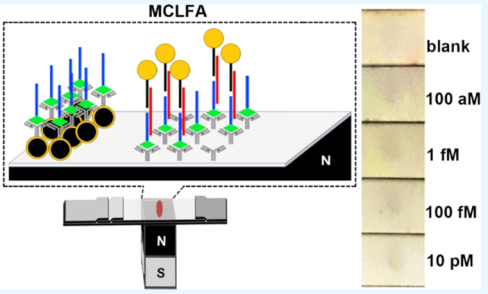

INTRODUCTION

Lateral flow assay (LFA) is an attractive analytical technique that is simple, robust, rapid, and cost-effective. The signal could be read by naked eyes, and hence most LFA systems do not require any extra instrumentation, making it attractive for on-site and point-of-care applications. In addition to the detection of protein targets for pathogens,[1−5] LFA has also been used for detecting nucleic acid targets.[6−9] However, the application of LFA to detect nucleic acid target sequences are limited due to poor sensitivity. To overcome the limitations, various strategies were proposed primarily to amplify the signal from LFA. Nanoparticle labeling is the most common strategy used for signal enhancement given the high extinction coefficient of nanoparticles which makes the colorimetric signal (from gold nanoparticles) stronger and easier for recognition by naked eyes.[10−12] With the nanoparticle-based probe sequences, silver or copper staining techniques have been used for signal amplification in LFA.[13−15] The enzymatic reaction which could catalyze the colorimetric reaction has also been applied to amplify the colorimetric signal.[16−18] Beyond the signal enhancement strategies mentioned above, few studies have attempted to increase the capture efficiency of the targets in the test zone of lateral flow (LF) strips to improve sensitivity. It has been reported that the capture efficiency on LF strips in conventional LFA could be less than 5%,[19] implying that the detection sensitivity of LFA could be improved if the capture efficiency can be increased. In the past, strategies based on the optimization of the nitrocellulose membrane were proposed by patterning pillars in the test zone of LF strips, as well as an electrophoresis-based technique termed isotachophoresis (ITP) to reduce the flow speed of the reagents in the LF strip for improved detection.[19−23] Our group have also reported a magnetic focus enhancement strategy to tune the movement and spatial distribution of labeled targets in the LFA and have applied this strategy to detect targets ranging from pathogenic cells, proteins, or nucleic acid sequences.[2,24−26] The magnetic focus enhancement combined with horseradish peroxidase amplified colorimetric signal yielded a 10^6-fold improvement in protein and 1 fM DNA sequence target detection. Here, the magnetic force between the magnetic nanoparticle probes and an external magnet provides a simple way to control the flow of sample components in the LFA requiring minimal additional materials compared with the conventional LFA. It should also be noted that the magnetic focus-enhanced LFA contains an enzymatic amplification step for colorimetric signal generation, which contributes not only to the improved sensitivity but also to the complexity of probe preparation and additional steps in signal generation, along with suitable conditions for the stability of enzymes immobilized onto the magnetic probes

Received: May 25, 2022
Accepted: August 1, 2022
Published: August 11, 2022

which could result in a possible variation in the enzyme activity when subjected to varying different storage/operating conditions. In spite of the limitations, a strong demand for simple, rapid, and sensitive technologies for nucleic acid sequence detection exists.

For the LFA detection of nucleic acid sequences, two technical routes have been reported: (i) the capture sequences immobilized at the test zone would specifically hybridize with the labeled target sequences in the sample flow.[27,28] In this approach, capture sequences need not be added to the sample solution. However, the hybridization time is limited during the sample flow where the labeled targets may pass the capture sequences immobilized on the LF strip, resulting in very low capture efficiency; or (ii) the target sequences are first hybridized with labeled probe sequences and the labeled capture sequences in the sample solution will give rise to a sandwich structure with label A-probe sequence/target sequence/capture sequence-label B where label A contributes to signal generation due to nanoparticles or enzyme and label B is used for target capture by the corresponding recognition ligands immobilized on the LF strips at the signal generation zone. The specificity of identification of target sequences is due to hybridization between the probe sequence, target sequence, and capture sequence. This route enables a longer incubation time for the hybridization between the capture sequence and target sequence and would result in the capture of more target sequences. The corresponding LF strip preparation would be simpler because it is easier to immobilize biotin or antibody on the strips compared with the immobilization of DNA capture sequences. However, it should be noted that to recognize as many target sequences as possible, the labeled probe sequences and capture sequences should be present at a much higher concentration than that of target sequences in the sample. As a result, besides the generated sandwich structures, there would still be a large number of unreacted label B-capture sequences. Furthermore, due to their smaller size, the unreacted label B-capture sequences would move faster than the sandwich structures, especially when label A is a nanoparticle. Thus, the unreacted label B-capture sequences would occupy the recognition ligands immobilized at the test zone of LF strips, and the capture efficiency of the sandwich structures would be decreased. LFA-based detection of nucleic acid sequences with a sandwich structure could be a very promising detection technique that simplifies the LF strip preparation enabling a more efficient hybridization with target sequences. Reducing the occupation of recognition ligands by unreacted CS-label would be critical for nucleic acid target detection using this approach.

In the present work, magnetic nanoparticles termed magnetic controllers were introduced to reduce the movement of unreacted CS-labels to minimize their presence/interference at the signal generation zone to result in enhanced detection sensitivity due to the capture of an increased number of sandwich structures with target sequences rather than the unreacted CS-label on LF strips. The magnetic controllers were constructed with Au/Fe_3O_4 core−shell nanoparticles modified with anti-FITC antibodies, which would interact with the fluorescein isothiocyanate (FITC) label on capture sequences. Meanwhile, gold nanoparticles (GNPs) modified with the probe sequences depicted as the gold probes (Gprobes) would hybridize with target sequences for signal. FITC-labeled capture sequences (CS−FITC) were used to generate Gprobe/target sequence/CS−FITC constructs. During the sample flow, the magnet under the LF strip would reduce the movement of magnetic controllers in the LF strip which are bound with the unreacted CS−FITC. Thus, the sandwich structure would reach the test zone first and allow for an increased interaction time and higher capture efficiency due to the anti-FITC antibodies on the test zone of the LF strips. Based on the GNP-based colorimetric signal which is presented as dots on the LF strip, the proposed MCLF could recognize as low as 100 aM of target sequences by naked eyes without any extra instrumentation or enzymatic amplification. The simplicity and cost of the MCLF procedure conceptualized are comparable to LFA techniques routinely used for detection, exhibiting a strong potential for on-site detection of targets at detection limits not possible before.

EXPERIMENTAL SECTION

Chemicals and Reagents. $HAuCl_4{\cdot}XH_2O$, tris(2-carboxyethyl)phosphine hydrochloride (TCEP), sodium citrate, sodium carbonate, ferric chloride, and ferrous chloride were purchased from Sigma-Aldrich (Missouri). Sodium hydroxide was obtained from Mallinckrodt Chemicals (New Jersey). Sodium borohydride was obtained from ACROS ORGANICS (New Jersey). Anti-FITC antibody (ABIN6391433) was purchased from antibodies-online Inc. (Pennsylvania). DNA sequences comprising capturing sequence (CS), probing sequence (PS), and target sequence (TS) were obtained from IDT DNA Technologies (Iowa). Model sequences designed for detection are as follows: (i) CS−FITC: GGC CAA TGT TTG TAA TCA GTT CCT TTT TTT TTT/36-FAM/, (ii) SH−PS: /5ThioMC6-D/TT TTT TTT TTT CCA TGC CAA TGC GCG ACA T, and (iii) TS: GGA ACT GAT TAC AAA CAT TGG CCG CAA ATT GCA CAA TTT GCC CCC AGC ATG TCG CGC ATT GGC ATG GA. The tubes with DNA powder were first centrifuged at 10 000 rpm for 10 min to precipitate all the powder to the bottom of the tube. A calculated volume of DI water was then added to the tubes and shaken for 30 min and kept overnight to prepare the DNA stock solution. The concentration of the stock solution at 100 μM was determined with a nanodrop instrument based on the OD at 260 nm. The dilutions were prepared by adding 10 μL of DNA solution to 990 μL of phosphate-buffered saline (PBS). All of the materials and chemicals were used as obtained without purification. Glasswares were cleaned with fresh aqua regia and rinsed with DI water.

Synthesis of Gold Nanoparticles and Magnetic Nanoparticles. Gold nanoparticles were synthesized based on the method reported by Frens.[29] Briefly, to 100 mL of boiling DI water, 1 mL of 1% $HAuCl_4{\cdot}XH_2O$ was added, followed by a rapid injection of 0.5 mL of 1% sodium citrate. The solution quickly changed from colorless to wine red. The obtained solution was kept to boiling for 15 min and cooled to room temperature. The GNP solution was stored at 4 °C until further use.

Fe_3O_4/Au core−shell magnetic nanoparticles, used as magnetic controllers, were synthesized based on our previous works.[2,25,26] To develop Fe_3O_4 nanoparticles, 3 mL of 1 M sodium hydroxide was added to 27 mL of DI water. The mixture was then heated to boiling and 2 mL of 0.4 M sodium citrate was added. After boiling the solution again, 1 mL of 0.4 M ferric chloride and 1 mL of 0.2 M ferrous chloride were rapidly added to the solution at the same time under strong stirring. The solution will undergo a rapid color change from

https://doi.org/10.1021/acsomega.2c03276
ACS Omega 2022, 7, 29204−29210

Scheme 1. Schematics of Conventional LFA and MCLFA for DNA Detection Based on TS-Containing Sandwich Structures

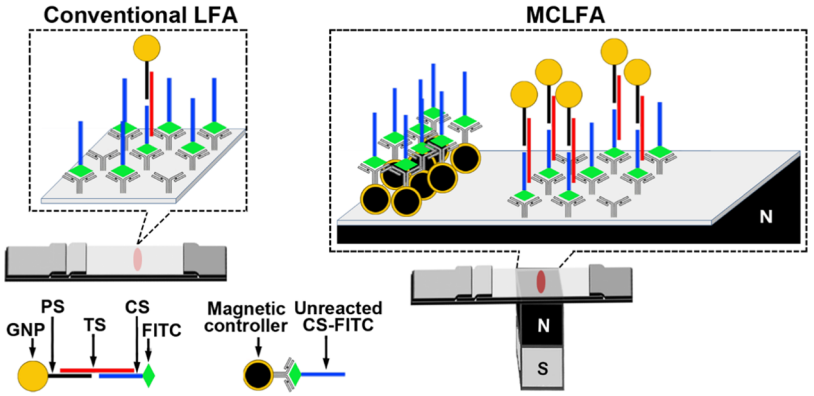

colorless to black immediately after the addition of ferric chloride and ferrous chloride. The obtained solution was then refluxed in the air for 4 h. The prepared Fe_3O_4 nanoparticles were purified three times with ethanol and water and redispersed in 10 mL of DI water.

The generation of Au shells around the Fe_3O_4 cores was performed as follows. A solution was prepared by mixing 920 μL of DI water and 80 μL of Fe_3O_4 nanoparticles and sonicated for 10 min. After centrifuging at 500 rpm for 10 min, 980 μL of supernatant was added with 100 μL of 1% $HAuCl_4$ and sonicated again for 10 min. Then, 200 μL of 10 mM freshly prepared ice-cold sodium borohydride was injected into the solution and kept under sonication for 10 min. The obtained Fe_3O_4/Au magnetic nanoparticles were washed three times with DI water and kept at 4 °C until further use.

The ultraviolet−visible (UV−vis) spectra of GNPs and Fe_3O_4/Au magnetic nanoparticles were recorded with a NanoDrop 1000 spectrophotometer (ThermoFisher Scientific Inc., Massachusetts). The size and concentration of GNPs and magnetic nanoparticles (NPs) were determined according to the report from Haiss et al.[30]

Preparation of Gprobes and Magnetic Controllers. The gold probes (Gprobes) were modified with SH−PS to specifically hybridize with the TS and then blocked with casein to minimize nonspecific binding. Briefly, 10 μL of 1 mM TCEP was mixed with 970 μL of DI water and then added to 20 μL of 100 μM SH−PS and kept at room temperature for 1 h. Then, 4 mL of GNP solution was centrifuged at 7000 rpm for 6 min, and the precipitate was added to the SH−PS solution. After mixing well, the solution was kept at room temperature for 48 h. To the solution, 100 μL of 10 × PBS was added, followed by the injection of 4 μL of 0.5 M sodium carbonate. The resulting solution was kept at room temperature for 24 h and then added to 110 μL of 5% casein and kept overnight. The solution was centrifuged and washed with DI water twice and redispersed in 1 mL of 1 × PBS; it was then added to 4 μL of 0.5 M sodium carbonate and 100 μL of 5% casein. The resulting solution was mixed well and kept at room temperature for 24 h; it was then washed three times with 0.5% casein in 1 × PBS and redispersed in 0.4 mL of 0.5% casein in 1 × PBS.

Magnetic nanoparticles termed magnetic controllers were constructed with magnetic nanoparticles (NPs) modified with anti-FITC antibodies. In 0.5 mL of magnetic NP solution, 2 μL of 0.5 M sodium carbonate and 10 μL of 1 mg/mL anti-FITC antibody solution were added. The obtained mixture was shaken at room temperature for 4.5 h. Then, 55 μL of 5% casein was added to the solution. After incubating at room temperature for 2.5 h, the solution was centrifuged and the obtained magnetic probes were centrifuged and washed with 0.5% casein in 1 × PBS twice and then redispersed in 200 μL of 0.5% casein in 1 × PBS.

Test of DNA Target. Lateral flow strips were assembled as described in our previous works.[2,24,25,31] Anti-FITC antibodies were dropped in the middle of the nitrocellulose membrane, and the strips were dried at 37 °C for 40 min.

To test the model DNA target (TS), Gprobes and 1 μL of 1 μM CS−FITC were added to 100 μL of TS in the PBS solution. After mixing well, the solution was incubated at room temperature for 15 min. Then, magnetic controllers were added to the solution. The solution was applied to the LF strips kept on a magnet rack. After 10 min of flow, the strips were washed with 60 μL of DI water once, and the strips can be imaged to indicate the color change at the signal generation zone on the strip for detection. To obtain quantitative values, the images were processed with ImageJ (National Institutes of Health), with the brightness and contrast normalized. Quantitative information from the images was calculated from the grayscale values of the deepest color from the dots generated on the LF strips minus the average grayscale value of the background area of the LF strips. The error bars show the deviation of the quantitative value from three replications.

RESULTS AND DISCUSSION

In conventional LFA, to detect target nucleic acid sequences based on the sandwich structure, samples with targets would first be mixed with labeled PS and CS which are usually kept at a high concentration to guarantee the hybridization with as many TS as possible in the sample. When the mixture is loaded to the LF strip, a high concentration of unreacted CS-label can be expected, possibly as high as 10^6-fold compared with the amount of TS. As shown in Scheme 1, these unreacted CS-labels would be captured by the antibodies immobilized on the LF strip, thus occupying the recognition ligands to decrease the capture efficiency of the TS-containing sandwich structures to result in poor sensitivity. Furthermore, these tend to reduce the capture efficiency of the TS-containing sandwich structures to result in poor sensitivity. It should be noted that, compared with the sandwich structures, the labeled CS has a smaller size and less mass and hence will have a higher mobility when introduced on the LF strip. These CS probes will reach the test zone before the sandwich structures bearing the TS and contribute to false positives by binding to the target sites at the test zone. This is one of the primary reasons for unsatisfactory

https://doi.org/10.1021/acsomega.2c03276
ACS Omega 2022, 7, 29204−29210

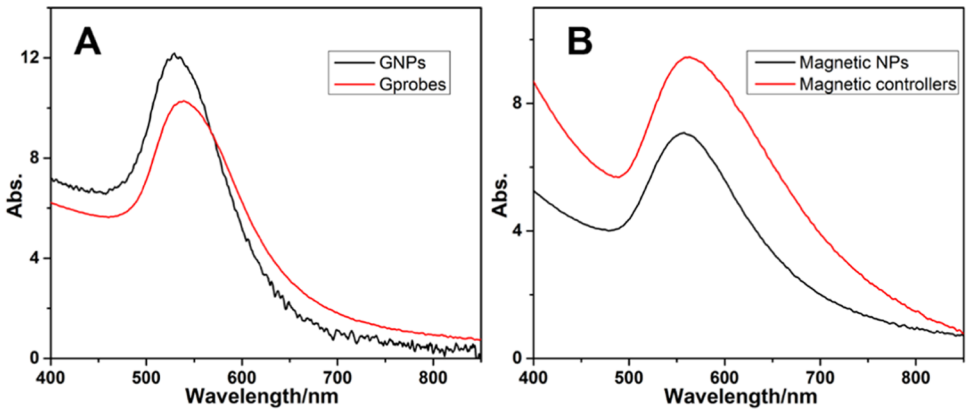

Figure 1. UV−vis spectra of (A) GNPs and Gprobes and (B) magnetic NPs and magnetic controllers.

sensitivity in the conventional LFA systems used for nucleic acid sequence detection.

In our previous work, with the magnetic focus-enhanced LFA approach, we have demonstrated that utilizing the magnetic field by a simple magnet the movement of the sample components when bound to functionalized magnetic NPs in the LF strip could be controlled to improve the limit of detection.[26] By extending this concept, when magnetic NPs were modified with recognition ligands to target the label (anti-FITC antibody in this work) on CS, the magnetic nanoprobes (i.e., magnetic controllers) would interact with the unreacted CS−FITC and flow at a reduced speed due to the magnetic field, allowing the TS-containing sandwich structures to reach the test zone and interact with the recognition ligands, resulting in improved capture efficiency and thereby a better detection sensitivity.

To demonstrate the modification of Gprobes and magnetic controllers, the UV−vis spectra of the nanoparticles before and after modification were recorded. As shown in Figure 1A, compared with GNPs, the UV−vis spectrum of Gprobes showed a wider peak width in addition to a redshift in the peak position, which demonstrates the modification of GNPs with PS. An extension in peak width and shift in peak position was also observed in the spectrum of functionalized magnetic probes compared with magnetic NPs, which confirmed the surface modification with the antibody.

To investigate the influence of the amount of antibodies on LF strips, 1 μL of 0.6 and 1 mg/mL antibodies were applied on LF strips, respectively. In the same MCLF test procedure, as shown in Figure 2, it can be seen that 1 fM of target provided an observable dot on the LF strip with 1 mg/mL of antibody, while no signal (depicted by a dot) was generated on the strip with 0.6 mg/mL of antibody for the same 1 fM of TS tested. As discussed above, in conventional LFA, the unwanted presence of the unreacted CS−FITC would influence the detection sensitivity. When the concentration of antibodies at the test zone of the LF strip is high, the opportunity to capture higher TS-containing sandwich structures is increased to result in better sensitivity. The amount of Gprobes is determined by the labeling efficiency of the incubation. To optimize the amount of Gprobes, MCLF tests with 1 fM of TS with varying concentrations of Gprobes were conducted and the corresponding results are shown in Figure 2. It can be seen that the presence of 1 fM of TS with 3 μL of Gprobes generated a signal (presence of a dot), while tests with 1 and 2 μL of Gprobes did not generate a signal (absence of a dot on the LF strip). Our results indicated that during incubation more TS-containing sandwich structures would be generated with increased concentration of Gprobes in the samples. Therefore, incubation with increased Gprobes would result in more Gprobes-linked constructs at the test zone of LF strips, resulting in a stronger signal. Magnetic controllers which would interact with the unreacted CS−FITC in the test played a key role in reducing the mobility of the unreacted CS−FITC so that a lower number of such probes are present at the test zone. To investigate the effect of the magnetic controllers on the detection results, varying levels of magnetic controllers were added to the sample solution and the detection results are as shown in Figure 2. The results show that there is no notable signal (depicted by a dot) on the strip when 0.5 μL of magnetic controllers are added to the sample solution, suggesting that the control from the magnetic controllers to the unreacted CS−FITC is insufficient and there is still an ample number of unreacted CS−FITC bound to the recognition ligands at the test zone. When 1 μL of magnetic controllers are added, the dot can be observed on the LF strips, demonstrating the magnetic control enhancement due to the detection sensitivity. With 1.5 μL of magnetic controllers, the

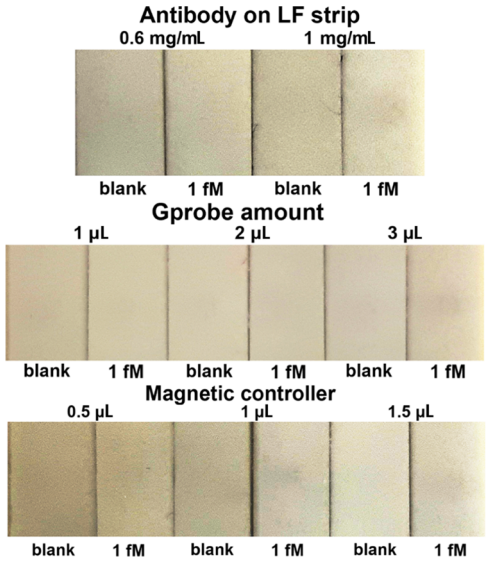

Figure 2. Results of optimization of antibodies immobilized on LF strips, Gprobe (C_{Gprobe} = 0.41 ± 0.07 nM) amount, and magnetic controller amount ($C_{magnetic\_controller}$ = 0.20 ± 0.05 nM) with PBS as blank and 1 fM TS in the PBS solution.

https://doi.org/10.1021/acsomega.2c03276
ACS Omega 2022, 7, 29204−29210

detection results from 1 fM TS are similar to those with 1 μL of magnetic controllers, suggesting the saturation of magnetic controllers to bind with the unreacted CS−FITC.

To demonstrate the enhancement from magnetic controllers, conventional LFA was performed with optimized concentration of Gprobes, where anti-FITC antibodies rather than anti-FITC antibody-modified magnetic controllers were added to the sample solution upon incubation to interact with the unreacted CS−FITC. It can be seen in Figure 3 that with

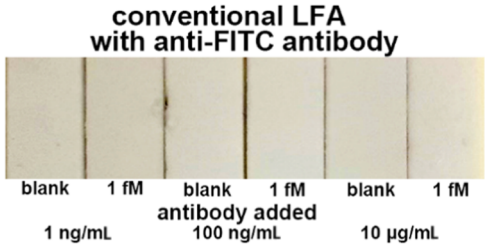

Figure 3. Results of conventional LFA with the addition of anti-FITC antibody to interact with unreacted CS−FITC.

an increased amount of antibody, there was no notable signal (dot) on the LF strips when 1 fM of TS was used as the test sample, indicating no enhancement when the antibody itself was added. Although the added antibody could also interact with the unreacted CS-FITC compared with the antibodies conjugated on magnetic NPs, the affinity between free antibodies and unreacted CS−FITC would be much lower compared to the antibodies conjugated onto the magnetic controller.[32] Therefore, we assess that the free antibodies will interact with the unreacted CS−FITC to a lesser extent compared with the antibodies conjugated to magnetic nanoparticles, resulting in a much weaker improvement due to the interaction between the free antibodies and unreacted CS−FITC than that with the magnetic controllers. Compared to the detection results shown in Figure 2, the negative results from conventional LFA with added antibody demonstrated that rather than the antibody interaction, the reduced mobility (due to the magnetic field) of the unreacted CS−FITC bound to magnetic controllers is a key reason for improved sensitivity. To exclude the steric-hindrance effect from the magnetic controllers, detection with the optimal level of Gprobes and magnetic controllers was performed with 1 fM TS with and without the magnet, respectively. As shown in Figure 4, it can

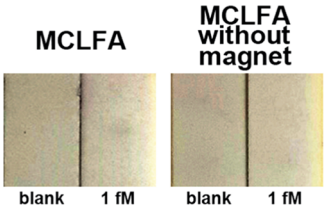

Figure 4. Results of the MCLFA test of blank PBS and 1 fM TS with and without the external magnet.

be seen that without the magnetic field, no signal was observed on the LF strip. In contrast, in the MCLF with the magnet, the appearance of the dot on the LF strip indicated the presence of 1 fM TS. The comparison shown in Figure 4 confirmed that the steric effect of magnetic NPs would not improve the detection results. Based on the results shown in Figures 3 and 4, in the proposed MCLF, the enhancement due to the detection sensitivity should be attributed to the reduced mobility of the unreacted CS−FITC bound probes with the magnetic controllers.

To demonstrate the detection capability of the proposed MCLF, TS at serial concentrations was tested. Typical results of LF strips were recorded in the inset image in Figure 5. It can

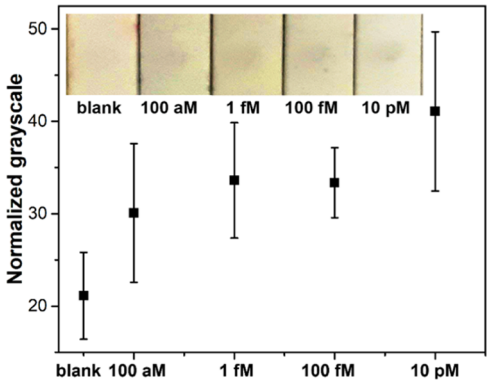

Figure 5. Plots based on normalized grayscales from the MCLFA test of blank, 100 aM, 1 fM, 100 fM, and 10 pM of TS. The inset shows a typical image of the LF strips after testing for the TS at serial concentrations.

be seen that a dot on the LF strip corresponding to the 100 aM concentration of TS was noted, while the color of the dots from the tests of 1 fM is slightly stronger than that from 100 aM. It should also be noted that the color from 1 and 100 fM is similar. The dot could still be obtained from 10 pM of TS, indicating a responding range from 100 aM to 10 pM. The quantitative value of the normalized grayscale of the dots on the LF strips was obtained from the difference between the grayscale value of the deepest color in the dot region and the average grayscale value of the background region on the same strip. The quantitative results from different concentrations are plotted in Figure 5, along with the error bars for the deviation shown from three replications. It can be seen that there is a clear increase in the normalized grayscale value from blank to 100 aM, indicating a detection sensitivity of as low as 100 aM TS in the PBS solution. Meanwhile, it should also be noted that the increase in the normalized grayscale value from 100 aM to 100 fM is not significant; only a slight increase in normalized grayscale from 100 fM to 10 pM was noted. In the proposed MCLF, the magnetic control enhancement became weaker when the concentration of TS increased. When TS is present at a high concentration in the sample, after sufficient incubation TS-containing sandwich structures are generated, while fewer unreacted CS−FITC are left in the sample solution resulting in less unwanted occupation. The magnetic controllers would interact with fewer unreacted CS−FITC, and the enhancement from the magnetic controllers becomes insignificant when the TS concentration is high. The proposed MCLF technique conceptualized exhibited excellent sensitivity; however, further work is needed to demonstrate the quantification of the TS.

CONCLUSIONS

In this work, an LFA-based detection strategy termed MCLF was proposed for nucleic acid sequence detection. Magnetic NPs modified with anti-FITC antibodies were used as

https://doi.org/10.1021/acsomega.2c03276
ACS Omega 2022, 7, 29204−29210

magnetic controllers to bind with the unreacted CS−FITC targets which would occupy the recognition ligands on the LF strip, thus reducing the capture efficiency of TS. With the magnetic field provided by a simple magnet, the movement of the unreacted CS−FITC bound with the magnetic controllers would be reduced; thus, the TS-containing sandwich complex would first arrive at the test zone to interact with the antibodies to increase capture efficiency. Utilizing model DNA sequence targets, with the proposed MCLF technique as low as 100 aM of TS could be detected by naked eyes without signal amplification. Based on our experiments, the response range of the MCLF was estimated to be from 100 aM to 10 pM of TS. The proposed MCLF has exceptionally high sensitivity and will make it possible to detect very low levels of targets by the colorimetric signal which was not possible before in a rapid format without any amplification products.

AUTHOR INFORMATION

Corresponding Author

Joseph Irudayaraj − *Department of Bioengineering, Holonyak Micro and Nanotechnology Laboratory; Beckman Institute; Carl Woese Institute for Genomic Biology, and Cancer Center at Illinois (CCIL), University of Illinois at Urbana—Champaign, Urbana, Illinois 61801, United States; Biomedical Research Center in Mills Breast Cancer Institute, Carle Foundation Hospital, Urbana, Illinois 61801, United States;* orcid.org/0000-0002-0630-1520; Email: jirudaya@illinois.edu

Author

Wen Ren − *Department of Bioengineering, University of Illinois at Urbana—Champaign, Urbana, Illinois 61801, United States; Biomedical Research Center in Mills Breast Cancer Institute, Carle Foundation Hospital, Urbana, Illinois 61801, United States*

Complete contact information is available at: https://pubs.acs.org/10.1021/acsomega.2c03276

Notes

The authors declare no competing financial interest.

ACKNOWLEDGMENTS

We appreciate the Jump Arches Seed grant program from the Health Care Engineering Center for partial funding of this work and the Cancer Center at Illinois at the University of Illinois at Urbana-Champaign. This research is also partly supported by the U.S. Department of Agriculture, Agricultural Research Service, under Project No. 59-8072-6-001. Any opinions, findings, conclusions, or recommendations expressed in this publication are those of the author(s) and do not necessarily reflect the view of the U.S. Department of Agriculture.

REFERENCES

(1) Cho, I. H.; Bhunia, A.; Irudayaraj, J. Rapid pathogen detection by lateral-flow immunochromatographic assay with gold nanoparticle-assisted enzyme signal amplification. *Int. J. Food Microbiol.* **2015**, *206*, 60−66.

(2) Ren, W.; Irudayaraj, J. Paper-Based Test for Rapid On-Site Screening of SARS-CoV-2 in Clinical Samples. *Biosensors* **2021**, *11*, No. 488.

(3) Zhang, D.; Huang, L.; Liu, B.; Ni, H. B.; Sun, L. D.; Su, E. B.; Chen, H. Y.; Gu, Z. Z.; Zhao, X. W. Quantitative and ultrasensitive detection of multiplex cardiac biomarkers in lateral flow assay with core-shell SERS nanotags. *Biosens. Bioelectron.* **2018**, *106*, 204−211.

(4) Duan, D. M.; Fan, K. L.; Zhang, D. X.; Tan, S. G.; Liang, M. F.; Liu, Y.; Zhang, J. L.; Zhang, P. H.; Liu, W.; Qiu, X. G.; Kobinger, G. P.; Gao, G. F.; Yan, X. Y. Nanozyme-strip for rapid local diagnosis of Ebola. *Biosens. Bioelectron.* **2015**, *74*, 134−141.

(5) Jiang, X.; Lillehoj, P. B. Lateral flow immunochromatographic assay on a single piece of paper. *Analyst* **2021**, *146*, 1084−1090.

(6) Rodriguez, N. M.; Linnes, J. C.; Fan, A.; Ellenson, C. K.; Pollock, N. R.; Klapperich, C. M. Paper-Based RNA Extraction, in Situ Isothermal Amplification, and Lateral Flow Detection for Low-Cost, Rapid Diagnosis of Influenza A (H1N1) from Clinical Specimens. *Anal. Chem.* **2015**, *87*, 7872−7879.

(7) Varona, M.; Eitzmann, D. R.; Anderson, J. L. Sequence-Specific Detection of ORF1a, BRAF, and ompW DNA Sequences with Loop Mediated Isothermal Amplification on Lateral Flow Immunoassay Strips Enabled by Molecular Beacons. *Anal. Chem.* **2021**, *93*, 4149−4153.

(8) Jain, S.; Dandy, D. S.; Geiss, B. J.; Henry, C. S. Padlock probe-based rolling circle amplification lateral flow assay for point-of-need nucleic acid detection. *Analyst* **2021**, *146*, 4340−4347.

(9) Wei, H. J.; Peng, Y. J.; Bai, Z. K.; Rong, Z.; Wang, S. Q. Duplex-specific nuclease signal amplification-based fluorescent lateral flow assay for the point-of-care detection of microRNAs. *Analyst* **2021**, *146*, 558−564.

(10) Yen, C.-W.; de Puig, H.; Tam, J. O.; Gómez-Márquez, J.; Bosch, I.; Hamad-Schifferli, K.; Gehrke, L. Multicolored silver nanoparticles for multiplexed disease diagnostics: distinguishing dengue, yellow fever, and Ebola viruses. *Lab Chip* **2015**, *15*, 1638−1641.

(11) Khlebtsov, B. N.; Tumskiy, R. S.; Burov, A. M.; Pylaev, T. E.; Khlebtsov, N. G. Quantifying the Numbers of Gold Nanoparticles in the Test Zone of Lateral Flow Immunoassay Strips. *ACS Appl. Nano Mater.* **2019**, *2*, 5020−5028.

(12) Li, D. Q.; Huang, M.; Shi, Z. Y.; Huang, L.; Jin, J. N.; Jiang, C. X.; Yu, W. B.; Guo, Z. Y.; Wang, J. Ultrasensitive Competitive Lateral Flow Immunoassay with Visual Semiquantitative Inspection and Flexible Quantification Capabilities. *Anal. Chem.* **2022**, *94*, 2996−3004.

(13) Panferov, V. G.; Safenkova, I. V.; Varitsev, Y. A.; Drenova, N. V.; Kornev, K. P.; Zherdev, A. V.; Dzantiev, B. B. Development of the sensitive lateral flow immunoassay with silver enhancement for the detection of *Ralstonia solanacearum* in potato tubers. *Talanta* **2016**, *152*, 521−530.

(14) Liu, C. C.; Yeung, C. Y.; Chen, P. H.; Yeh, M. K.; Hou, S. Y. *Salmonella* detection using 16S ribosomal DNA/RNA probe-gold nanoparticles and lateral flow immunoassay. *Food Chem.* **2013**, *141*, 2526−2532.

(15) Tian, M.; Lei, L.; Xie, W.; Yang, Q.; Li, C. M.; Liu, Y. Copper deposition-induced efficient signal amplification for ultrasensitive lateral flow immunoassay. *Sens. Actuators, B* **2019**, *282*, 96−103.

(16) Cho, I. H.; Bhandari, P.; Patel, P.; Irudayaraj, J. Membrane filter-assisted surface enhanced Raman spectroscopy for the rapid detection of *E. coli* O157:H7 in ground beef. *Biosens. Bioelectron.* **2015**, *64*, 171−176.

(17) He, Y. Q.; Zhang, S. Q.; Zhang, X. B.; Baloda, M.; Gurung, A. S.; Xu, H.; Zhang, X. J.; Liu, G. D. Ultrasensitive nucleic acid biosensor based on enzyme-gold nanoparticle dual label and lateral flow strip biosensor. *Biosens. Bioelectron.* **2011**, *26*, 2018−2024.

(18) Adhikari, M.; Dhamane, S.; Hagstrom, A. E. V.; Garvey, G.; Chen, W. H.; Kourentzi, K.; Strych, U.; Willson, R. C. Functionalized viral nanoparticles as ultrasensitive reporters in lateral-flow assays. *Analyst* **2013**, *138*, 5584−5587.

(19) Moghadam, B. Y.; Connelly, K. T.; Posner, J. D. Two orders of magnitude improvement in detection limit of lateral flow assays using Isotachophoresis. *Anal. Chem.* **2015**, *87*, 1009−1017.

(20) Rivas, L.; Medina-Sanchez, M.; de la Escosura-Muniz, A.; Merkoci, A. Improving sensitivity of gold nanoparticle-based lateral

flow assays by using wax-printed pillars as delay barriers of microfluidics. *Lab Chip* **2014**, *14*, 4406−4414.
(21) Tang, R.; Yang, H.; Gong, Y.; Liu, Z.; Li, X.; Wen, T.; Qu, Z.; Zhang, S.; Mei, Q.; Xu, F. Improved analytical sensitivity of lateral flow assay using sponge for HBV nucleic acid detection. *Sci. Rep.* **2017**, *7*, No. 1360.
(22) Rosenfeld, T.; Bercovici, M. 1000-fold sample focusing on paper-based microfluidic devices. *Lab Chip* **2014**, *14*, 4465−4474.
(23) Moghadam, B. Y.; Connelly, K. T.; Posner, J. D. Isotachophoretic preconcenetration on paper-based microfluidic devices. *Anal. Chem.* **2014**, *86*, 5829−5837.
(24) Ren, W.; Ahmad, S.; Irudayaraj, J. 16S rRNA Monitoring Point-of-Care Magnetic Focus Lateral Flow Sensor. *ACS Omega* **2021**, *6*, 11095−11102.
(25) Ren, W.; Cho, I.-H.; Zhou, Z.; Irudayaraj, J. Ultrasensitive detection of microbial cells using magnetic focus enhanced lateral flow sensors. *Chem. Commun.* **2016**, *52*, 4930−4933.
(26) Ren, W.; Mohammed, S. I.; Wereley, S.; Irudayaraj, J. Magnetic focus lateral flow sensor for detection of cervical cancer biomarkers. *Anal. Chem.* **2019**, *91*, 2876−2884.
(27) Rastogi, S. K.; Gibson, C. M.; Branen, J. R.; Eric Aston, D.; Larry Branen, A.; et al. DNA detection on lateral flow test strips: enhanced signal sensitivity using LNA-conjugated gold nanoparticles. *Chem. Commun.* **2012**, *48*, 7714−7716.
(28) Henderson, W. A.; Xiang, L.; Fourie, N. H.; Abey, S. K.; Ferguson, E. G.; Diallo, A. F.; Kenea, N. D.; Kim, C. H. Simple lateral flow assays for microbial detection in stool. *Anal. Methods* **2018**, *10*, 5358−5363.
(29) Frens, G. Controlled nucleation for regulation of particle-size in monodisperse gold suspensions. *Nat. Phys. Sci.* **1973**, *241*, 20−22.
(30) Haiss, W.; Thanh, N. T. K.; Aveyard, J.; Fernig, D. G. Determination of size and concentration of gold nanoparticles from UV-Vis spectra. *Anal. Chem.* **2007**, *79*, 4215−4221.
(31) Ren, W.; Ballou, D. R.; FitzGerald, R.; Irudayaraj, J. Plasmonic enhancement in lateral flow sensors for improved sensing of *E. coli* O157: H7. *Biosens. Bioelectron.* **2019**, *126*, 324−331.
(32) Safenkova, I. V.; Zherdev, A. V.; Dzantiev, B. B. Correlation between the composition of multivalent antibody conjugates with colloidal gold nanoparticles and their affinity. *J. Immunol. Methods* **2010**, *357*, 17−25.

https://doi.org/10.1021/acsomega.2c03276
ACS Omega 2022, 7, 29204−29210